Article

Not peer-reviewed version

Seed Endophyte *Bacillus atrophaeus* Colonizes Root and Shoot Tissues Providing Antifungal Activity During Wheat Seedling Establishment

Anagha Wankhade *, Zhiting Xu, Ashlynn Ellexa Clark, David Britt *

Posted Date: 31 March 2026

doi: 10.20944/preprints202603.2503.v1

Keywords: *Bacillus atrophaeus*; seed endophyte; wheat microbiome; seed-to-surface transition; biofilm formation; antifungal activity; rhizosphere colonization; biosurfactant; biological control

 doi:10.20944/preprints202603.2503.v1

Article

Seed Endophyte *Bacillus atrophaeus* Colonizes Root and Shoot Tissues Providing Antifungal Activity During Wheat Seedling Establishment

Anagha Wankhade [1,*], Zhiting Xu [2], Ashlynn Ellexa Clark [1] and David Britt [1,*]

[1] Department of Biological Engineering, Utah State University, Logan, UT, USA

[2] College of Science, University of Utah, Salt Lake City, UT, USA

* Correspondence: anagha.wankhade@usu.edu (A.W.); david.britt@usu.edu (D.B.)

Abstract

Seed-associated endophytes become active during germination, playing important roles as early colonizers of plant tissues, contributing to plant health while residing in a protective niche. In this study, we characterized a wheat-derived bacterial isolate, JunSE1L, to determine its functional traits and ecological role in the plant microbiome. The isolate was identified as *Bacillus atrophaeus* based on 16S rRNA analysis. JunSE1L exhibited nutrient-dependent plasticity in colony architecture, forming robust hydrophobic biofilms and pellicles under rich nutrient availability, while swarming and forming thin, often dendritic colonies under defined nutrition. JunSE1L produced highly surface-active compounds that lowered the surface tension of water to 30 mN/m and released potent proteolytic and hemolytic compounds, thus equipping JunSE1L for offensive roles, as examined against several fungal pathogens. JunSE1L inhibited *Fusarium proliferatum* and *Mucor hiemalis* in live-cell assays, while cell-free supernatant selectively inhibited *M. hiemalis*. JunSE1L was recovered from multiple plant compartments, including rhizosphere, rhizoplane, and aerial tissues, and was observed to emerge from cut plant tissues, supporting seed-endophyte mobilization upon germination to colonize distal tissues. Seed surface inoculation experiments with JunSE1L showed limited attachment at low cell densities and reduced seedling vigor at higher inoculum levels, supporting agricultural approaches nurturing the existing seed microbiome.

Keywords: *Bacillus atrophaeus*; seed endophyte; wheat microbiome; seed-to-surface transition; biofilm formation; antifungal activity; rhizosphere colonization; biosurfactant; biological control

1. Introduction

Seed-associated endophytes are important contributors to early plant microbiome assembly and seedling establishment. Because they are already present at germination, these microorganisms can colonize emerging roots and shoots and influence microbial community development during early plant growth. Seed endophytes can also persist throughout the plant life cycle and may be transmitted across plant generations through both vertical and horizontal transmission routes, thereby shaping plant-associated microbiomes over time [1–3]. Consequently, seed-associated microbial communities represent an important reservoir of early colonizers capable of influencing plant health, stress tolerance, and interactions with surrounding microbial communities, presenting a sustainable and organic alternative to agrochemicals for these conditions.

Members of the genus *Bacillus* are among the most frequently recovered seed-borne and plant-associated bacteria across diverse crops, including cereals and quinoa [4–6]. Their success in plant-associated environments is partially attributed to the formation of stress-resistant endospores, which allow survival under desiccation, nutrient limitation, and temperature fluctuations typical of soil and aerial plant habitats [7,8]. In addition, many plant-associated *Bacillus* strains produce extracellular hydrolytic enzymes and membrane-active lipopeptides such as surfactin, iturin, and fengycin. These

 doi:10.20944/preprints202603.2503.v1

metabolites contribute to microbial competition and suppression of plant pathogens through mechanisms including antibiosis, niche competition, and activation of plant defense responses [9–12].

Successful colonization of plant surfaces requires adaptation to highly heterogeneous environmental conditions. The rhizosphere and phyllosphere exhibit strong spatial and temporal variation in nutrient availability, moisture, and abiotic stress, which shapes associated microbial communities [13,14]. In *Bacillus*, environmental conditions such as nutrient composition, osmotic stress, temperature, and water potential regulate colony architecture, extracellular matrix production, biofilm formation, and sporulation. Changes in nutrient availability or polymeric substrates can alter biofilm structure, hydrophobicity, and colony morphology, while osmotic stress can shift populations between motile and sessile states [15–17]. Biofilm development – including pellicle formation at the air-liquid interface – enhances persistence, surface attachment, and tolerance to environmental stress by embedding cells within an extracellular polymeric matrix [18,19]. Biosurfactants such as surfactin reduce surface tension and facilitate spreading motility, thus promoting stable colonization of plant surfaces and the induction of systemic resistance (ISR) in plants [15,20–22]. Biosurfactants also coat hydrophobic surfaces, including air bubbles, potentially preventing embolisms in the xylem [23], which worsen under drought conditions [24].

Through their persistence on plant surfaces, many plant-associated *Bacillus* strains contribute to plant health through direct antifungal activity. This antagonism is commonly mediated by secreted lipopeptides and related metabolites that disrupt fungal membranes, inhibit spore germination and hyphal growth, and suppress disease development in plants [25,26]. Lipopeptides such as iturins, fengycins, bacillomycins, and mycosubtilin can damage fungal membranes by altering ergosterol-dependent membrane integrity, causing leakage of cellular contents and growth inhibition. These properties underpin broad-spectrum suppression of phytopathogenic fungi and have led to the widespread use of *Bacillus*-based formulations as biological control agents in agriculture [27–29].

Despite the well-recognized role of *Bacillus* in plant health, most mechanistic studies have focused on rhizosphere-derived isolates or on individual functional traits examined in isolation, such as lipopeptide production or enzymatic activity [30]. Less attention has been given to how multiple adaptive traits – including nutrient-dependent developmental plasticity, biofilm formation, biosurfactant production, persistence strategies, and antifungal activity operate together within a single seed-derived isolate. Understanding how seed endophytes integrate these traits to transition from seed-associated microbes to active plant surface colonizers therefore remains an important gap in our understanding of plant–microbe interactions.

Crop yields are often compromised by abiotic stress (e.g., drought) that often increases plant susceptibility to biotic stressors, such as fungal pathogens. This study focused on two ecologically distinct fungal targets: *Fusarium proliferatum* and *Mucor hiemalis*. *Fusarium* species are among the most important fungal pathogens affecting cereal crops and are associated with seedling disease, root and crown rot, and mycotoxin contamination. In contrast, *Mucor* species are fast-growing saprophytic fungi commonly found in soil and plant-associated environments. Testing antagonism against both organisms, therefore allows evaluation of bacterial antifungal activity across distinct fungal groups relevant to both plant pathology and soil microbial communities.

In this study, a bacterial endophyte was isolated from surface-sterilized wheat seeds and designated JunSE1L (Juniper Seed Endophyte isolate 1, large-colony variant). Preliminary phenotypic characteristics suggested affiliation with the genus *Bacillus*. We hypothesized that a seed-derived isolate exhibiting strong environmental plasticity and surface-associated traits could transition into a functional epiphyte with antifungal potential. To test this hypothesis, we (i) identified the isolate using 16S rRNA gene sequencing, (ii) evaluated its ability to colonize wheat root and shoot surfaces, (iii) characterized nutrient-dependent phenotypic plasticity and persistence-related traits – including colony architecture, hydrophobicity, biofilm and pellicle formation, sporulation, extracellular enzyme production, and biosurfactant activity – and (iv) assessed antifungal activity against *Fusarium proliferatum* and *Mucor hiemalis*. Together, these experiments

 doi:10.20944/preprints202603.2503.v1

were designed to determine whether a seed-borne *Bacillus* isolate can transition into a plant-associated surface colonizer with traits relevant to biological control.

2. Materials and Methods

2.1. Endophyte Isolation

Seeds of winter wheat (Triticum aestivum, var. Juniper, developed by the Idaho Agriculture Experiment Station as a stress-tolerant cultivar (https://digitalcommons.usu.edu/grcanyon/235/), collected from a 2020 organically grown harvest, were surface sterilized by immersion in 100 ml of 10% hydrogen peroxide (H_2O_2) (Sigma-Aldrich, Cat. No. 516813) in 250 mL for 10 min with constant shaking. Seeds were added in a single layer covering the bottom of the flask to ensure uniform exposure to the sterilizing solution. After extensive washing in sterile distilled water, the seeds were transferred to 2% Lysogeny Broth (LB) agar plates. The plates were sealed with Parafilm™ and incubated at 22 °C for 4 d. Inoculum, removed from the colonies growing around the surface of the wheat seeds, was transferred into sterile water and serial dilutions were plated onto 2% LB agar. Purification of the single colonies growing on these plates utilized the three-streak method, which produced two stable cultures that yielded either large or small colonies when grown on 2% LB. These cultures were termed JunSE1L for the large colony form and JunSE1S for the small colony cell type. Cells were maintained in 15% glycerol at -75 °C. The studies in this paper involved the endophyte JunSE1L, which is the large colony phenotype.

2.2. Colonization of Wheat Roots and Shoots by Seed Endophyte JunSE1L

2.2.1. Seed Surface Sterilization and Plant Growth

Wheat seeds were surface sterilized by immersion in 10% H_2O_2, same as explained above, followed by three rinses with sterile distilled water. To verify the effectiveness of sterilization, seeds were placed on LB (2% agar; medium consisted of tryptone (Fisher BioReagents, Cat. No. BP1421), yeast extract (Fisher BioReagents, Cat. No. BP1422), and no added salt) plates and incubated for 24 h to check for microbial growth.

Magenta™ boxes were prepared using sterile sand (Granusil 4075). Sand was washed and dry-sterilized at 200 °C for 14 h. 20 × 6 × 6 cm Magenta ™ boxes were disinfected with 70% ethanol, filled with 300 g sterile sand, and supplemented with 50 mL sterile distilled water. The sand was mixed and fluffed using ethanol-sterilized tools before sowing. Surface-sterilized seeds, with no visible surface microbial growth, were planted in Magenta™ plant growth boxes (3 seeds/box) and grown for 6 days at 22 ˚C.

2.2.2. Assessment of Rhizosphere, Rhizoplane, and Phyllosphere Colonization

After 6 days, plants were harvested under sterile conditions in a biosafety cabinet. Seedlings were transferred onto sterile aluminum foil for processing.

Rhizosphere colonization: Sand adhering to roots was collected and transferred into sterile 15 mL tubes. Sterile distilled water was added at a ratio of 1 mL per 0.1 g sand and vortexed. 100 µL suspensions were plated onto LB (2% agar) to observe any bacterial growth.

Rhizoplane colonization: Roots were immersed in 10 mL sterile distilled water and vortexed for 1 min to detach surface-associated bacteria. 100 µL of the root wash was plated onto LB (2% agar). In addition, root segments were excised, gently cleaned of residual sand using sterile forceps, and placed directly onto LB plates to assess bacterial emergence from root tissues.

Phyllosphere colonization: Leaves were cut and plated directly onto LB (2% agar) plates to determine bacterial emergence from internal tissues.

All plates were incubated at 22 °C and monitored for colony development. Colony morphology was used as a preliminary indicator of strain identity when recovering bacteria from plant tissues.

 doi:10.20944/preprints202603.2503.v1

2.3. Endophyte Emergence from Cut Plant Tissues on Agar

Surface-sterilized seeds (as described above) were placed directly onto 2% LB agar plates and incubated at 22 °C under sealed conditions (Parafilm™). Seedlings were allowed to grow for five days without transfer to sand systems.

At day 5, roots and shoots were aseptically cut using 70% ethanol-sterilized tweezers inside a biosafety cabinet. Plates were resealed and returned to incubation at 22 °C. Emergence of bacterial colonies from the cut ends of plant tissues was monitored over time, and images were captured at regular intervals to document endophyte growth.

2.4. Characterization of Endophyte JunSE1L for the Production of Bacillus sp. Traits

The isolate JunSE1L was examined for its production of features characteristic of authentic Bacillus isolates. Traits examined were production of surfactants [31], hydrophobin [32–34], and spores, as well as hemolysis [35] and extracellular protease [36] activities.

Production of hydrophobin and spores

Hydrophobin production was assessed with colonies formed on LB or MM 2% agar surfaces. Mature colonies of JunSE1L were established by inoculation of the agar plates with 10 µl of stationary phase cells (OD_{600} of 0.5) suspended in sterile distilled water. These cells, from cultures grown in LB or MM broths to the stationary phase with shaking at 140 rpm at 22 °C, were pelleted by centrifugation and resuspended in sterile distilled water. These sealed agar plate cultures were incubated for 15 d, and then a 5 µl drop of distilled water was placed on a colony. Images of the drop were taken within a minute. The stability of the drop was timed up to 2 hours.

Spore production was studied by staining using the Schaeffer-Fulton technique [37]. Briefly, a bacterial smear on a glass slide was air-dried and heat fixed. The sample was flooded with malachite green (Millipore Sigma, USA) and steamed for 5 min. After rinsing with distilled water, the sample was counterstained with safranin (Millipore Sigma, USA) for 30 sec, rinsed, and heat-fixed before being observed under a 100X objective.

2.4.1. Production of Pellicles

JunSE1L cells were initially pre-grown in a liquid minimal medium. Following the pre-growth phase, the cells were washed twice with distilled water to remove any residual medium. Subsequently, 100 µL of the washed cell suspension was transferred into separate flasks containing 100 mL of either minimal medium or LB medium. The cultures were incubated on a bench top at 22 °C without shaking. To monitor the growth and behavior of the cells, pictures were taken at regular time intervals throughout the incubation period.

2.4.2. Determination of Hemolysis Activity

The hemolysis activity of isolates was determined by noting zones of clearing around the colonies formed after bacteria were inoculated onto agar plates containing 5% sheep blood (Columbia blood agar, Hardy Diagnostics). The JunSE1L cells were grown in LB at 22 °C with shaking at 140 rpm to mid-logarithmic phase before being washed in sterile water. Suspensions of the JunSE1L cells in sterile distilled water were applied in 10 µl aliquots (OD_{600} of 0.5) in triplicate to the blood agar plate. Growth was recorded at 30 °C.

2.4.3. Extracellular Protease Activity

Secretion of extracellular protease by JunSE1L was examined by observing zones of clearing around bacterial colonies growing on plates of Skim Milk Agar (SMA) medium (Medallion Milk Co.) at 30 °C [38].

 doi:10.20944/preprints202603.2503.v1

2.4.4. Assessment of Phosphate Solubilization and Nitrogen Fixation

JunSE1L was grown by inoculating 100 µL of stock culture into 50 mL of minimal medium and incubating at 22 °C with shaking at 140 rpm for 48 h. The culture optical density (OD_{600}) was adjusted to 0.5. Cells were harvested by centrifugation at 16,000 × g for 10 min, washed twice with sterile distilled water, and resuspended in distilled water.

Aliquots (20 µL) of the washed cell suspension were spotted onto Pikovskaya agar (HiMedia) to assess phosphate solubilization and onto Norris glucose nitrogen-free medium (2% agar, HiMedia) to evaluate nitrogen-fixing ability. Plates were incubated at 22 °C and monitored for colony growth and the formation of clearance zones around colonies.

2.4.5. Production of Surfactants

Surfactant production by JunSE1L was assessed over time during growth in a minimal medium (MM) broth. The minimal medium [39] contained buffered potassium phosphate (pH 7) (MP Biomedicals, Cat. No. 151946, Fisher Chemicals, Cat. No. P285), citrate (Mallinckrodt Chemicals, Cat. No. 0754-12), and sucrose (Mallinckrodt AR, Cat. No. 8360) as carbon sources, and ammonium sulfate (Fisher Chemicals, Cat. No. A702) and magnesium sulfate (Fisher Scientific, Cat. No. M63) as the primary nitrogen, magnesium, and sulfur sources. Cultures were grown with shaking at 140 rpm at 22 °C. At defined time intervals between 14 and 48 h, growth was examined by measuring the OD_{600} nm of three samples of the culture. At the same time, three 1 ml aliquots were aseptically removed and centrifuged at 10,000 g for 10 min. The pelleted cells were discarded and the supernatant was filtered through a 0.22 µm filter. The surface tension of the filtrate was measured using a tensiometer (a wire probe tensiometer from Kibron Instruments, Malminkaari, Helsinki, Finland). As controls for each sample, the surface tension of double-distilled sterile water and of absolute ethanol were measured. The temperature for these assays was 22 °C.

Partial purification of the surfactants involved precipitation at pH 2 followed by solubilization at pH 7 (Płaza et al. 2015). Culture filtrates of JunSE1L on MM grown for 3 d were adjusted to pH 2 by the addition of concentrated hydrochloric acid. After 14 h, the mixture was centrifuged at 10,000 g for 30 min, and the supernatant was removed by decantation. 5 ml of distilled water and 5 ml of 0.2 M NaOH were added to the pellet to bring the mixture to pH 7. After vortexing for 2 min, the solution was frozen at -80 °C for 16 h and lyophilized over 24 h. The mass of the flaky white product was used as the partially purified surfactant. The critical micelle concentration (CMC) of the isolated biosurfactant was determined from serial dilutions of a stock of 10 mg/ml of the pH 2-precipitated material. Subsequently, the surface tension of each dilution was measured using the tensiometer. The CMC was identified from the dilution after which no further changes in surface tension occurred.

2.4.6. Molecular Identification of the Seed Endophyte JunSE1L

To identify the endophyte, JunSE1L, a sample was incubated on a streaked plate of the bacteria for two days and a single colony was isolated in 1 ml of autoclaved distilled water, then boiled for 5 minutes, lysing the cells and releasing DNA. Once boiled and centrifuged to collect supernatant, the DNA was subjected to PCR. The PCR recipe was taken directly from the Master mix's protocol, GoTaq Green by Promega and combined with primers centered on the 16S rRNA region of the bacterial genome. Specifically, 27F16S (5' AGAGTTTGATCMTGGCTCAG 3') and 1492R (5' CGGTTACCTTGTTACGACTT 3') [40] were used in combination with the extracted bacterial DNA and GoTaq Green master mix. A Techne Prime Thermocycler was used with protocol obtained from GoTaq Green: initial denaturation at 95°C for 5 minutes, then 35 cycles of denaturation at 95°C for 30 seconds, annealing at 52°C for 1 minute, and extension at 72°C for 1 minute, with a final extension at 72°C for 10 minutes. Once the PCR product was retrieved, gel electrophoresis was performed to ensure a single, strong band persisted in the product. The gel matrix consisted of agarose and Tris-Borate-EDTA (TBE) buffer with ethidium bromide as a fluorescent dye, electrophoresed at 100V. After about 45 minutes, the gel was imaged using a BioRad GelDoc Go scanner with UV light. After

 doi:10.20944/preprints202603.2503.v1

ensuring proper DNA isolation, a New England Biolabs Monarch Spin PCR and DNA Cleanup Kit was used to clean and prepare the PCR product for sequencing according to the manufacturer's protocol. 12 µl of the supplied elution buffer was used to elute the DNA. Analysis for purity and concentration was done on a ThermoScientific NanoDrop One. The purified DNA was sent to Eton Bioscience for Sanger sequencing, and the sequence was identified using Basic Local Alignment Search Tool (BLAST), aligning against the NCBI nucleotide database. The sequence has been submitted to the NCBI GenBank database, and the accession number will be provided upon assignment.

2.5. Antifungal Activity of JunSE1L

2.5.1. Fungal Isolates and Molecular Identification

Fusarium proliferatum, a known pathogen of winter wheat, was obtained from the Utah Plant Pest Diagnostic Laboratory after isolation from a marble onion collected in Corrine, Utah. Another fungal isolate was included to assess broad-spectrum antifungal activity: recovered from infected turfgrass in Salt Lake County, Utah provided by the Utah Plant Pest Diagnostic Laboratory.

For molecular identification of the turfgrass-associated fungi, each isolate was grown on solid medium for 48 h. Mycelial material was collected using a sterile loop and transferred to 1.5 mL microcentrifuge tubes for DNA extraction. Genomic DNA was isolated using the DNeasy Plant Mini Kit (QIAGEN) following the manufacturer's protocol, with elution volumes reduced to 50 µL (two elutions).

The internal transcribed spacer (ITS) region was amplified using primers ITS5 (5′-GGAAGTAAAAGTCGTAACAAGG-3′) and ITS4 (5′-TCCTCCGCTTATTGATATGC-3′) with repliQa HiFi ToughMix (Quantabio). PCR cycling conditions consisted of 40 cycles of 95 °C for 10 s, 52 °C for 5 s, and 68 °C for 1 s. Amplicons were verified by agarose gel electrophoresis in TBE buffer containing ethidium bromide to visualize DNA and then purified using the Monarch PCR & DNA Cleanup Kit (New England Biolabs). Purified products were sequenced by Sanger sequencing (Eton Bioscience), and sequences were identified using BLAST against the NCBI nucleotide database.

2.5.2. Antifungal Activity Assay

Frozen stocks of JunSE1L (15% glycerol) were revived in 50 mL LB and incubated at 22 °C with shaking (140 rpm). Cultures were subcultured once into fresh LB and grown for 24 h. Cells were harvested and adjusted to OD_{600} = 0.5 using fresh LB. The culture was centrifuged at 16,000 × g for 10 min, and the pellet was washed once and resuspended in sterile distilled water for use in antifungal assays.

Fungal inocula were prepared by suspending actively growing mycelial material in sterile distilled water and vortexing to obtain a uniform suspension. Aliquots (100 µL) of the fungal suspension were spread evenly onto LB agar plates (2% agar) and allowed to dry under sterile conditions.

A 10 µL drop of the OD-adjusted JunSE1L suspension was placed at the center of each fungal plate. Control plates received a 10 µL drop of sterile distilled water applied to the agar surface. Plates were incubated at 22 °C for 4 days and examined for zones of reduced fungal growth surrounding the bacterial inoculation site.

2.5.3. Antifungal Activity of Cell-Free Culture Supernatant

To assess the contribution of extracellular metabolites, JunSE1L was grown in LB for 48 h under the conditions described above. Cultures were centrifuged twice at 4,000 × g for 20 min to remove cells, and the supernatant was filtered through a 0.22 µm membrane to obtain sterile cell-free culture supernatant. Sterility of the filtrate was confirmed by plating an aliquot onto LB agar.

Sterile 6 mm Grade 1 Whatman filter paper disks were immersed in the supernatant for 15 s and placed onto fungal lawns prepared as described above. Control disks were soaked in sterile distilled

 doi:10.20944/preprints202603.2503.v1

water for the same duration. Plates were incubated at 22 °C for 4 days and examined for inhibition zones surrounding the disks.

2.6. Seed Surface Inoculation Assay

Surface-sterilized wheat seeds (as described above) were inoculated with JunSE1L to evaluate its potential for seed biopriming. Bacterial suspensions were prepared in sterile distilled water at approximately 10^4 and 10^8 CFU mL^{-1}. Seeds were immersed in the respective suspensions under static conditions to allow surface attachment. Seeds in the 10^4 CFU mL^{-1} treatment were incubated for 10 and 30 min, while seeds in the 10^8 CFU mL^{-1} treatment were incubated for 10 min.

Following inoculation, individual seeds were removed using sterile tweezers and gently shaken to remove excess liquid. Residual droplets were further removed by briefly dabbing seeds on sterile Kimwipes(TM).

To quantify bacterial attachment, seeds from each treatment were transferred into 1 mL sterile distilled water and vortexed for 30 s to detach surface-associated cells. Serial dilutions were prepared, and 100 µL aliquots were plated onto LB agar to determine colony-forming units associated with each seed.

3. Results

3.1. Isolation of Juniper Wheat Seed Endophyte JunSE1L

White bacterial colonies emerged from approximately 80% (44 out of 55 seeds) of surface-sterilized seeds of the wheat cultivar Juniper when germinated on LB 2% agar (Figure 1A). Colony development was visually similar among most seeds and consisted of opaque white colonies with raised edges forming in close proximity to the seed. Bacterial growth was consistently observed surrounding the germinating seeds but was not detected when intact root or shoot tissues contacted the LB agar surface during early seedling development. Because these colonies arose from surface-sterilized seeds under sterile conditions, they were considered seed-associated endophytes.

Purification by streaking to single colonies on LB agar yielded two distinct colony morphologies. One morphology produced large, rugose colonies, while the second consisted of smaller, smoother colonies (Figure 1B). The large-colony isolate was designated JunSE1L (Figure 1C), and the smaller colony variant was termed JunSE1S (Figure 1D). Both colony morphologies were stable and retained through repeated transfers on LB agar. Subsequent characterization in this study focused on the JunSE1L isolate.

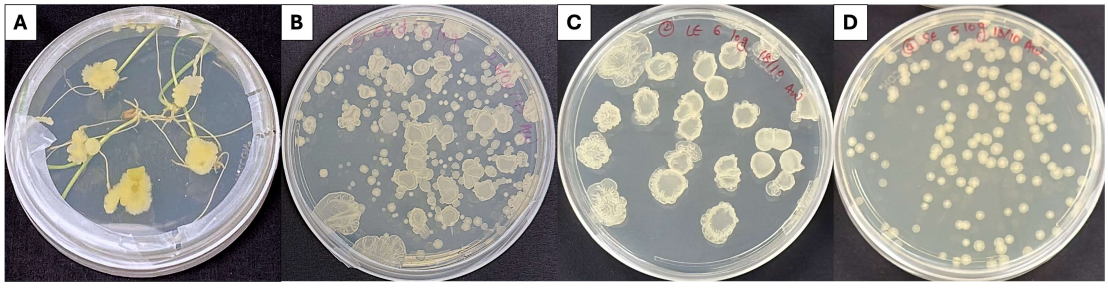

Figure 1. Isolation and colony morphology of bacteria emerging from surface-sterilized wheat seeds (cv. Juniper). (A) White bacterial colonies emerging from germinating wheat seeds with an emergence rate of 80% (44 out of 55 seeds) after 4 days of incubation on LB agar. (B) Colony morphology observed after dilution plating of bacteria recovered from a single seed shown in (A), revealing two distinct colony sizes. (C) Large, rugose colonies of the isolate designated JunSE1L after 4 days of growth on LB agar. (D) Smaller, smooth colonies of the isolate designated JunSE1S after 4 days of growth on LB agar. .

 doi:10.20944/preprints202603.2503.v1

3.2. Seed-Origin Endophyte Detected in Multiple Plant Compartments from Seedlings Grown in Sterile Sand

Colonies morphologically similar to JunSE1L were recovered from several plant-associated niches after six days of growth of surface-sterilized seeds in sterile sand in closed Magenta(TM) boxes. Bacteria were detected in the rhizosphere from sand adhering to the roots (Figure 2A). In rhizoplane assays, colony formation was observed from root wash suspensions and from plated root segments (Figure 2B, C), indicating the presence of bacteria associated with root surfaces or closely associated root tissues.

Colonies with morphology consistent with JunSE1L were also recovered from aerial plant tissues. Growth developed from leaf and shoot segments placed on LB agar after harvest (Figure 2D). Bacterial emergence was most frequently observed from cut edges of roots and shoots rather than from intact tissues. Colonies were rarely detected when intact plant surfaces were placed directly on agar.

Some variation in colony appearance compared with colonies emerging directly from germinating seeds (Figure 1A) was observed. This difference likely reflects variation in local moisture availability and surface drying of LB agar during incubation, conditions known to influence colony spreading, matrix production, and colony architecture in *Bacillus* biofilms [41,42].

To further confirm the internal origin of the endophyte, surface-sterilized seeds were also germinated directly on 2% LB agar plates without transfer to sand systems. After five days of growth, roots and shoots were aseptically cut using sterile tweezers. A JunSE1L-like endophyte consistently emerged from the cut ends of both roots and shoots, and its temporal emergence is documented in Figures S1 and S2.

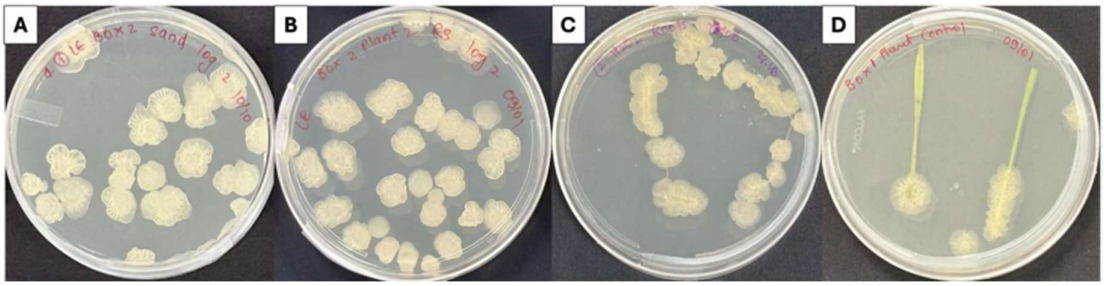

Figure 2. Recovery of JunSE1L-like colonies from harvested wheat tissues. (A) Bacterial colonies recovered from rhizosphere sand adhering to roots of seedlings grown from surface-sterilized seeds. (B) Colonies obtained from root wash suspensions indicating rhizoplane-associated bacteria. (C) Colony development from plated root segments following harvest. (D) Colonies emerging from leaf and shoot tissues placed on LB agar. In most cases, bacterial growth was observed from cut edges of plant tissues rather than intact surfaces. Colonies recovered from plant tissues displayed morphology consistent with the JunSE1L isolate when grown on LB medium. Experiments were conducted under sterile conditions as described in Methods. .

All assays were conducted under sterile conditions as described in the Methods, minimizing the possibility of external microbial contamination. Although colonies recovered from plant tissues displayed morphology consistent with JunSE1L, their identity in these assays was inferred based on colony morphology and was not confirmed by DNA-based identification. The consistent recovery of colonies with similar morphology from multiple plant compartments suggests that the seed-associated bacterium can persist during seedling growth and become detectable following tissue disruption during sample preparation.

3.3. Nutrient-Dependent Growth Plasticity of JunSE1L

JunSE1L displayed pronounced differences in colony morphology and development depending on nutrient conditions (Table 1). On LB agar (2% agar), colonies remained compact and wrinkled with limited lateral spreading. Colony diameter ranged from 1.1 ± 0.1 cm at day 3 to 1.5 ± 0.1 cm by

 doi:10.20944/preprints202603.2503.v1

day 7. In contrast, colonies grown on MM spread widely and exhibited a flatter morphology, reaching 2.4 ± 0.2 cm by day 3 and expanding to 4.1 ± 0.6 cm by day 5.

Colony surface hydrophobicity also differed between growth conditions. Water droplets applied to LB-grown colonies remained spherical for approximately 1.5 – 2 hours, indicating strong hydrophobicity. This phenotype appeared by day 3 and persisted through day 15. In contrast, droplets placed on MM-grown colonies flattened rapidly and were absorbed into the colony surface within approximately 10 minutes, indicating reduced hydrophobicity.

Sporulation timing also differed between the two media. In MM-grown colonies, spores within mother cells were first observed by day 5, and free spores were detected by day 7. In contrast, sporulation was delayed in LB-grown colonies, where spores within mother cells were first detected only after 15 days of incubation. Sporulation was assessed qualitatively by microscopic observation of malachite green-stained cells.

Together, these observations demonstrate strong nutrient-dependent developmental plasticity in JunSE1L, affecting colony architecture, surface properties, and sporulation dynamics.

Table 1. Nutrient-dependent changes in colony growth, surface hydrophobicity, and sporulation of JunSE1L on LB and minimal media.

Day	Hydrophobicity		Spore formation		Colony diameter (cm) (2% agar)	
	LB	MM	LB	MM	LB	MM
3	+	-	-	-	1.1 ± 0.1	2.4 ± 0.2
5	+	+/-	-	Within the mother cell	1.1 ± 0.0	4.1 ± 0.6
7	+	+/-	-	Free	1.5 ± 0.1	4.0 ± 0.5
9	+	+/-	-	Free	N/A	N/A
15	+	+/-	Within the mother cell	Free	N/A	N/A

*Hydrophobicity was assessed by observing droplet behavior on colony surfaces following application of sterile water. A "+" indicates formation of a stable nearly spherical droplet, while "+/–" indicates droplet flattening followed by absorption into the colony surface within approximately 10 minutes. Spore formation was detected using malachite green staining and categorized as spores within mother cells or free spores following release. Colony diameter represents the maximum colony dimension measured for colonies grown on agar surfaces.

3.4. Surface-Associated Growth and Biofilm Formation

Additional phenotypes supported a surface-associated lifestyle for JunSE1L. Colonies grown on LB developed a rugose morphology and strong colony surface hydrophobicity (Figure 3B), consistent with the production of surface-active or hydrophobic cell envelope components. In static liquid cultures, JunSE1L formed a thick pellicle at the air-liquid interface in LB within 48 h (Figure 3D), indicating robust biofilm formation.

In contrast, no visible pellicle or appreciable surface biomass developed in minimal medium under the same static conditions (Figure 3E), suggesting that biofilm formation in JunSE1L is enhanced under nutrient-rich conditions.

 doi:10.20944/preprints202603.2503.v1

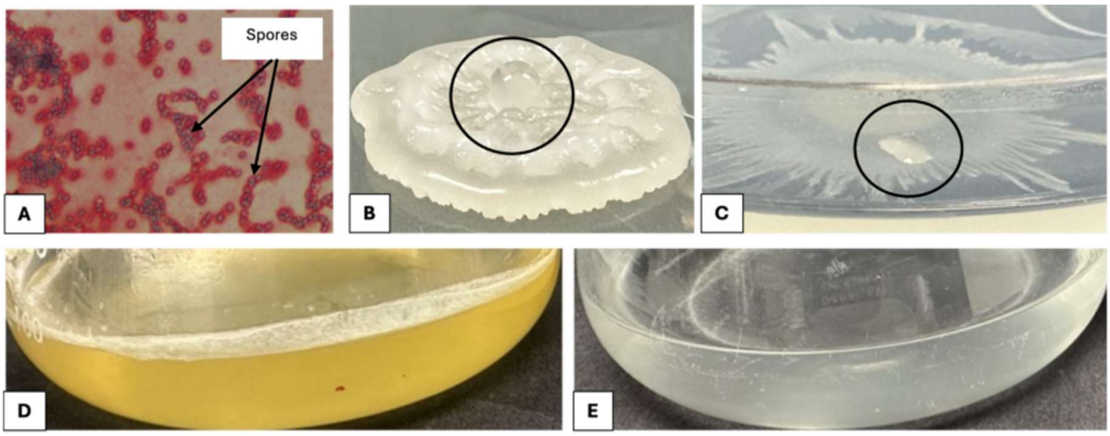

Figure 3. Surface-associated traits and biofilm formation in JunSE1L. (A) Spore production by JunSE1L after 15 days of incubation on LB agar (2% agar). Spores are stained green with malachite green (arrows), while vegetative cells are counterstained pink with safranin. (B) Hydrophobic colony surface after 3 days of growth on LB agar, demonstrated by retention of a nearly spherical water droplet for at least 2 hours. (C) Colony surface on MM agar after 7 days, where the water droplet flattened and was absorbed within 10 minutes, indicating reduced hydrophobicity. (D) Pellicle formation by JunSE1L after 48 h incubation in static LB medium, showing a thick biofilm at the air-liquid interface. (E) Absence of pellicle formation in minimal medium under identical static conditions. .

3.5. Extracellular Lytic Activities and Nutrient-Mobilization Traits

JunSE1L exhibited extracellular lytic activities when grown on diagnostic media. Colonies produced clear hemolytic zones on blood agar after 3 days of incubation, indicating hemolytic activity (Figure 4A). Growth on skim milk agar also resulted in zones of casein hydrolysis surrounding colonies, demonstrating secretion of extracellular proteases (Figure 4B).

In contrast, no zones of clearance were observed on Pikovskaya agar, indicating the absence of detectable phosphate-solubilizing activity under the conditions tested (Figure 4C). Similarly, growth on nitrogen-free medium did not indicate nitrogen-fixing capability (Figure 4D). Together, these observations suggest that JunSE1L lacks classical nutrient-mobilization traits but produces extracellular lytic activities commonly associated with microbial competition.

3.6. Production of Extracellular Biosurfactant

Growth of JunSE1L in liquid minimal medium resulted in a growth-phase-dependent reduction in surface tension of the culture filtrate. Surface tension decreased from 72.2 mN m^{-1} (pure water) to approximately 30 ± 0.01 mN m^{-1} by 38 h of growth (Figure 4E). The decline began at approximately 34 h and corresponded to the late exponential growth phase, during which cell density increased from an initial ~10^6 CFU mL^{-1} to 5 (±1) × 10^8 CFU mL^{-1}.

Surface-active compounds were recovered from cell-free culture supernatant by acid precipitation at pH 2 and retained activity after resuspension at neutral pH. Surface tension measurements of serial dilutions of the isolated material were used to estimate the CMC, which was approximately 0.125 mg mL^{-1} (Figure 4F). The gradual transition in surface tension across an order of magnitude of extract concentration suggests that multiple surface-active molecules may contribute to the observed reduction in surface tension

 doi:10.20944/preprints202603.2503.v1

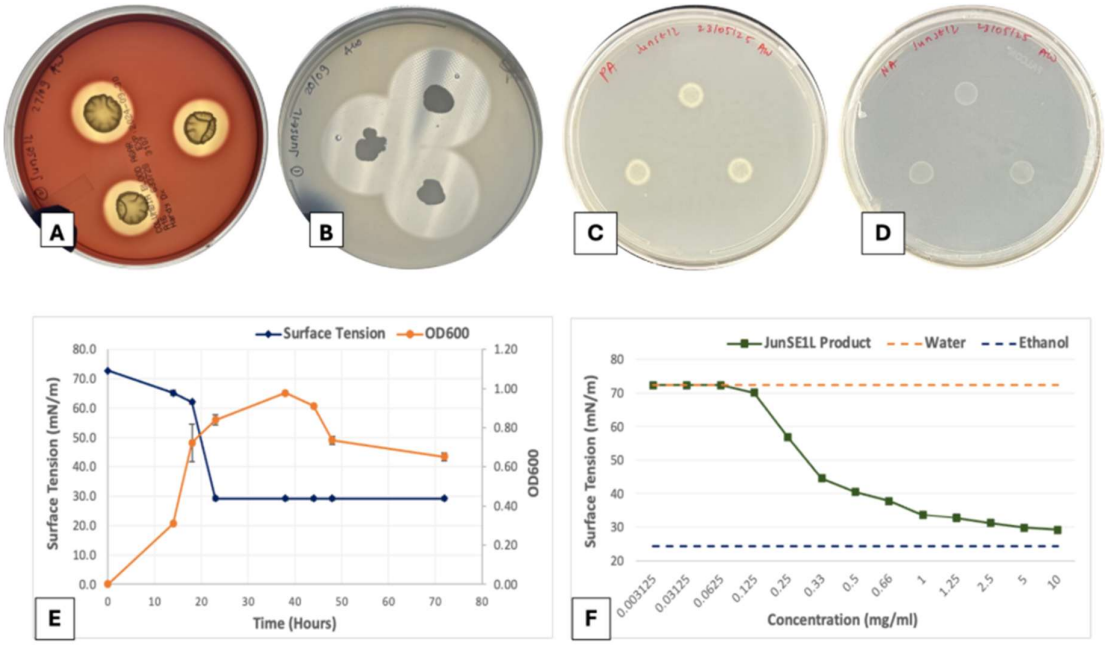

Figure 4. Extracellular lytic activities, nutrient-mobilization traits, and biosurfactant production by JunSE1L. (A) Hemolytic activity of JunSE1L on blood agar after 3 days of incubation, indicated by zones of clearing surrounding colonies. (B) Proteolytic activity on skim milk agar showing casein hydrolysis surrounding colonies after 3 days of growth. (C) Growth of JunSE1L on Pikovskaya agar showing no detectable phosphate-solubilizing activity under the conditions tested. (D) Growth of JunSE1L on nitrogen-free medium indicating absence of detectable nitrogen-fixing capability. (E) Relationship between bacterial growth (OD_{600}) and reduction in surface tension of culture supernatant during growth of JunSE1L in liquid minimal medium. Surface tension decreased from that of pure water to approximately 30 mN m^{-1} during late exponential growth. (F) Relationship between surface tension and concentration of the pH-2-precipitated biosurfactant fraction used to estimate the CMC. Error bars represent three biological replicates; values fall within the symbols. .

3.7. Molecular Identification of the Seed Endophyte JunSE1L

Phenotypic characteristics of JunSE1L – including colony morphology, sporulation, biosurfactant production, hemolytic activity, and extracellular protease secretion – suggested affiliation with the genus *Bacillus*. PCR amplification of the 16S rRNA gene followed by sequencing and BLAST analysis identified the isolate as *Bacillus atrophaeus* with 100% sequence identity. These results confirm that the seed-derived endophyte JunSE1L belongs to the species *Bacillus atrophaeus*.

3.8. Identification of Fungal Isolates Used in Antifungal Assays

Genomic DNA was isolated from the turfgrass-associated fungal isolate used in antifungal assays. Sequencing of the ITS region followed by BLAST analysis identified this isolate as *Mucor hiemalis* with 100% sequence identity. The wheat-associated fungal pathogen *Fusarium proliferatum* used in this study had been previously isolated and molecularly identified by the Utah Plant Pest Diagnostic Laboratory using the same ITS-based approach.

3.9. Antifungal Activity of JunSE1L

JunSE1L inhibited fungal growth when applied as a live bacterial suspension. When a 10 µL drop of the 0.5 OD_{600} bacterial suspension was placed at the center of plates inoculated with fungal lawns, clear zones of reduced fungal growth developed surrounding the bacterial inoculation site after 4 days of incubation at 22 °C. This inhibition was observed for both *Mucor hiemalis* and *Fusarium proliferatum* (Figure 5iA, 5iB), indicating antagonistic activity against both fungi.

 doi:10.20944/preprints202603.2503.v1

To determine whether extracellular metabolites contributed to this effect, sterile filter paper disks were dipped in cell-free culture supernatant of JunSE1L for approximately 15 s and then placed onto fungal lawns. Under these conditions, inhibition zones were observed around disks containing the JunSE1L supernatant for *Mucor hiemalis*, indicating the presence of diffusible antifungal compounds produced by JunSE1L. In contrast, no detectable inhibition was observed against *Fusarium proliferatum* when treated with the same supernatant (Figure 5iC, 5iD). Control treatments using sterile distilled water showed no inhibition of fungal growth. For disk controls, sterile filter paper disks were dipped in sterile distilled water for approximately 15 s before being placed on the agar surface, while additional controls received sterile distilled water applied directly to the agar surface (Figure 5iiA-D).

These results indicate that extracellular metabolites produced by JunSE1L contribute to antifungal activity against certain fungi, although their effectiveness appears to be species dependent.

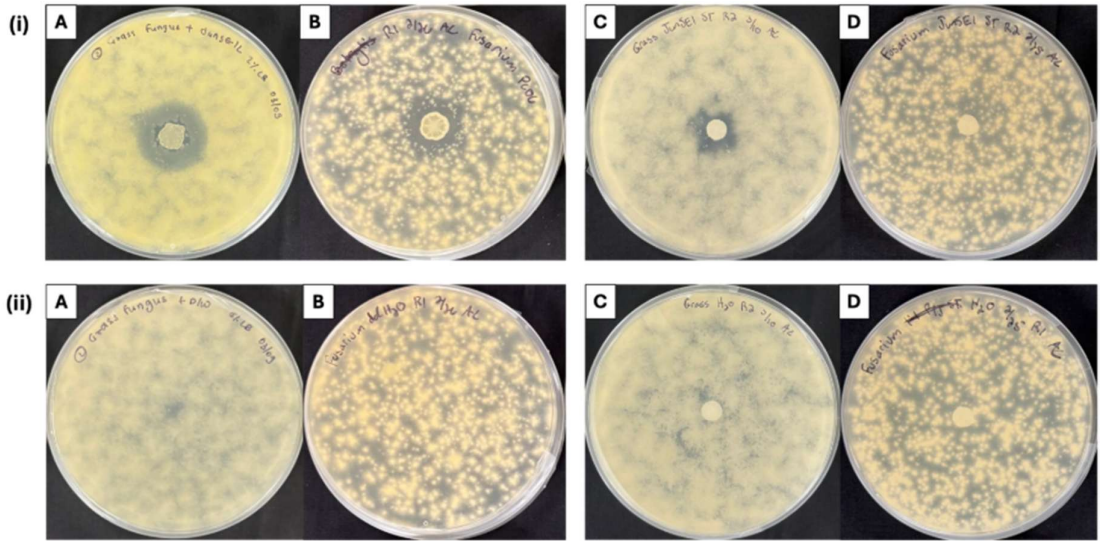

Figure 5. Antifungal activity of JunSE1L against *Mucor hiemalis* and *Fusarium proliferatum*. (i) Plates treated with live JunSE1L cells or cell-free culture supernatant. (ii) Corresponding sterile distilled water controls. (A, C) Assays with *Mucor hiemalis*. (B, D) Assays with *Fusarium proliferatum*. (A, B) A 10 µL drop of OD-adjusted JunSE1L suspension placed at the center of fungal lawns, showing inhibition of fungal growth after 4 days of incubation at 22 °C. (C, D) Sterile filter paper disks dipped in cell-free culture supernatant and placed on fungal lawns; inhibition was observed for *M. hiemalis* but not for *F. proliferatum*. (ii, A-D) Sterile distilled water controls applied either directly to the agar surface or using filter paper disks dipped in sterile distilled water. .

3.10. Limited Efficiency of Seed Surface Inoculation

To assess whether JunSE1L could be applied as a seed inoculant for biopriming applications, surface inoculation experiments were performed using two bacterial concentrations. At 10^4 CFU mL^{-1}, minimal to no bacterial attachment was detected on the seed surface following incubation, even after extended exposure times. In contrast, inoculation at 10^8 CFU mL^{-1} resulted in 10^5 CFU mL^{-1} bacterial recovery from seeds, indicating successful attachment at higher cell densities.

However, seeds treated with the higher inoculum exhibited reduced germination and early seedling vigor compared to controls when transferred to 2% LB medium. These results suggest that while increased bacterial concentration enhances surface colonization, it may negatively affect early plant development.

 doi:10.20944/preprints202603.2503.v1

4. Discussion

16S rRNA analysis identified the wheat-associated isolate JunSE1L as *Bacillus atrophaeus*, and physiological characterization revealed traits consistent with a stress-tolerant, surface-associated plant colonizer with antifungal potential. Members of the *Bacillus* genus are widely recognized for their ecological versatility, persistence through sporulation, and ability to suppress plant pathogens through biofilm formation and secretion of antimicrobial metabolites [43]. The functional profile observed for JunSE1L aligns with these characteristics and suggests that its ecological role in the wheat microbiome is primarily protective rather than nutritional.

The colony and pellicle phenotypes suggest that JunSE1L readily adopts a surface-associated lifestyle, with nutrient availability shaping whether the population remains in a biofilm state or shifts toward dormancy. In *Bacillus*, these transitions are governed by interconnected regulatory pathways that couple matrix production, multicellular behavior, and entry into [44–46]. The low surface tension of the culture supernatant is also consistent with lipopeptide biosurfactant production, which in *Bacillus* promotes surface spreading and accelerates pellicle development, while hydrophobin-like matrix components such as BslA can generate the hydrophobic barrier characteristic of mature biofilms [22,47–50]. Together, these traits support the idea that JunSE1L is well adapted to persist on exposed plant surfaces where fluctuating moisture, nutrient supply, and competition favor organized multicellular growth.

The antifungal phenotype further supports the interpretation that JunSE1L functions as a competitive surface colonizer. Inhibition was observed when live bacterial cells were applied to fungal lawns, indicating strong antagonistic activity at the site of bacterial growth. Cell-free culture supernatant also inhibited the grass-associated fungus *Mucor hiemalis* but did not produce detectable inhibition against *Fusarium proliferatum* under the same conditions. This result indicates that JunSE1L produces extracellular antifungal compound(s), while also suggesting that activity in the live-cell assay may be strengthened by local accumulation of these compounds near the bacterial colony or by additional cell-associated effects. Because the differential response was observed only in the supernatant assay, it is more conservative to interpret this pattern as assay-dependent or concentration-dependent variation in susceptibility rather than as evidence of strict target specificity. Such an interpretation is consistent with prior work showing that *Bacillus* lipopeptides, including iturins, fengycins, and surfactins, can differ in antifungal potency across fungal taxa and that their activity depends on membrane-level interactions and exposure conditions [35,51]. Biofilm matrices can further concentrate or transiently retain secreted products within structured communities, increasing their effective local activity near the colony surface [42,52].

From an ecological perspective, the inhibition of *M. hiemalis* may be particularly relevant to wheat because wheat belongs to the grass family (Poaceae) and interacts with fungi commonly present in soil and rhizosphere environments associated with grasses. As a fast-growing saprophytic fungus frequently found in soil, *M. hiemalis* may represent a relevant competitor or target organism encountered during early seedling establishment. Its sensitivity to JunSE1L supernatant may therefore better reflect interactions occurring in wheat-associated environments than does the response of *F. proliferatum* alone. At the same time, the lack of supernatant inhibition against *F. proliferatum* indicates that extracellular activity is not uniformly expressed across fungi and may depend on metabolite concentration, stability, diffusion through agar, or inherent differences in fungal susceptibility. Together, these observations support a model in which JunSE1L combines surface-associated growth with production of diffusible antifungal compounds, but whose measurable activity depends strongly on the biological context of the target fungus and the assay format used.

An important aspect emerging from this study is that the ecological role of JunSE1L should be interpreted in the context of the host plant rather than solely as an isolated antagonist. Although bacteria were not recovered from intact root or shoot tissues during early seed germination, colonies with morphology consistent with JunSE1L were later detected from rhizosphere, rhizoplane, and aerial plant compartments. Rather than representing a contradiction, this pattern may reflect a

 doi:10.20944/preprints202603.2503.v1

dynamic transition from a low-abundance or dormant seed-associated state to active colonization of plant surfaces during seedling establishment. Seed-associated microbes are increasingly recognized as contributors to early microbiome assembly, influencing rhizosphere and phyllosphere colonization even when initially present at low abundance [53,54]. Responses of *B. atrophaeus* and related species to root exudates further support this possibility, as these signals can promote sessile growth and surface colonization behaviors [55].

In the context of winter wheat, which undergoes vernalization and is exposed to prolonged low temperatures, the ability of JunSE1L to form spores and persist within seeds may be particularly advantageous. Sporulation enables survival under fluctuating and often harsh environmental conditions, allowing the endophyte to remain viable during cold periods and resume activity during germination. This trait may contribute to the stability of seed-associated microbiota and ensure early colonization of emerging seedlings. Furthermore, early emergence from seed-associated niches may position JunSE1L to compete with epiphytic microorganisms already present in the soil, thereby influencing microbial community assembly at the seed-soil interface.

From an applied perspective, these observations are particularly relevant to the use of *Bacillus* species as seed-priming agents in agriculture. *Bacillus* strains are commonly applied as spores or powder-based formulations to enhance seed colonization, improve germination, and provide early protection against soil-borne [56,57]. However, in this study, surface inoculation of wheat seeds with vegetative cells of JunSE1L was inefficient at lower concentrations and required high cell densities to achieve detectable attachment. Notably, these higher inoculum levels negatively affected seed germination and early seedling growth, indicating a trade-off between colonization efficiency and host compatibility. These results suggest that JunSE1L is more effectively transmitted through its natural seed-associated endophytic lifestyle than through external surface inoculation. Consistent with this interpretation, spore-based delivery systems or approaches that mimic natural seed association may be more suitable for establishing beneficial interactions without compromising plant development.

This perspective also helps explain the ecological function of JunSE1L during early plant development. As seedlings grow in soil, roots and shoots experience mechanical abrasion, micro-wounding, and interactions with soil microorganisms and microfauna. Such processes may release bacteria from protected internal seed-associated niches, allowing them to colonize newly exposed plant surfaces. Once established, these bacteria can occupy attachment sites, form biofilms, and interact directly with surrounding microbial communities. In this context, JunSE1L may function as a mobile defensive population originating from the seed endosphere and recruited to plant surfaces during early development, where it can contribute to microbial competition and pathogen suppression.

Beyond direct antagonism, many *Bacillus* species are also known to enhance plant immunity through ISR. Bacterial lipopeptides such as surfactin and fengycin can act as microbe-associated molecular patterns (MAMPS) that activate plant defense signaling pathways and prime plants for more rapid responses to pathogen attack [35,58]. Although ISR was not directly evaluated in this study, the biosurfactant-associated traits and stable surface colonization observed for JunSE1L suggest that its ecological contribution may include both localized pathogen suppression and stimulation of host defense responses—Indeed, this may have contributed to the selection of JunSE1L by ancestral host plants. Together, these findings support a model in which JunSE1L functions as a protective member of the wheat-associated microbiome, transitioning from seed association to surface colonization and contributing to host defense through persistence, biofilm formation, and antifungal activity.

5. Conclusions

This study identified JunSE1L, a seed-derived wheat endophyte, as *Bacillus atrophaeus* and showed that it exhibits multiple traits associated with plant-associated bacteria. JunSE1L displayed nutrient-dependent variation in colony architecture, hydrophobicity, sporulation, and biofilm

 doi:10.20944/preprints202603.2503.v1

formation. It formed rugose colonies, developed pellicles, produced biosurfactant activity with a low critical micelle concentration, and exhibited extracellular proteolytic and hemolytic activities.

JunSE1L was recovered from the rhizosphere, rhizoplane, and aerial tissues following seed germination. In antifungal assays, live cells inhibited both *Fusarium proliferatum* and *Mucor hiemalis*. Cell-free culture supernatant inhibited *M. hiemalis* but not *F. proliferatum* under the conditions tested, indicating the presence of diffusible extracellular compounds with activity dependent on assay conditions.

The traits observed in JunSE1L include features associated with microbial competition and persistence. These include offensive traits, such as antifungal activity and production of extracellular compounds, and defensive traits, such as sporulation, biofilm formation, and biosurfactant production that may contribute to survival and surface association.

Taken together, these findings support a model in which JunSE1L functions as a protective wheat-associated *Bacillus* that transitions from seed association to active colonization of plant surfaces, where it may contribute to microbial competition and pathogen suppression through both close-range interactions and secreted metabolites. Although *Bacillus* species are widely used as seed treatments in agriculture, our results indicate that direct surface inoculation through biopriming of wheat seeds with vegetative cells of JunSE1L, under the conditions tested, is inefficient at low concentrations and can negatively impact seedling development at higher inoculum densities. This suggests that leveraging its natural seed-associated endophytic lifestyle or developing spore-based delivery systems that better mimic this mode of trasmission, may be more effective for practical applications. The environmental plasticity, surface persistence, and antifungal activity of JunSE1L highlight its role in biological control.

Supplementary Materials: The following supporting information can be downloaded at the website of this paper posted on Preprints.org, Figure S1: Emergence of endophyte from cut shoot tissue; Figure S2: Emergence of endophyte from cut root tissue.

Author Contributions: Conceptualization, A.W. and D.W.; methodology, A.W. and D.W.; validation, A.W., and D.W.; formal analysis, A.W.; investigation, A.W., Z.X., and A.C; resources, D.W.; data curation, A.W., Z.X., and A.C; writing—original draft preparation, A.W.; writing—review and editing, A.W., A.C., and D.W.; visualization, A.W., and D.W.; supervision, D.W.; project administration, D.W.; funding acquisition, D.W. All authors have read and agreed to the published version of the manuscript.

Funding: This research was funded by USDA-NIFA Award 2024-67022-42830 and UAES Project UTAO-1581. The funding bodies had no role in the design of the study; collection, analysis, or interpretation of data; or in writing the manuscript.

Institutional Review Board Statement: Not applicable.

Informed Consent Statement: Not applicable.

Data Availability Statement: All data generated or analyzed during this study are included in this published article and its supplementary information files. Additional datasets supporting the conclusions of this article are available from the corresponding author upon reasonable request.

Acknowledgments: The authors thank members of the Britt Lab for helpful discussions and technical assistance. We are especially grateful to Dr. Anne Anderson for her constant support, insightful guidance, and fruitful scientific discussions throughout this study. We also thank Dr. Claudia Nischwitz from the Biology Department at Utah State University for providing fungal cultures for antifungal assays and for access to her laboratory facilities for DNA extraction of fungal isolates and the endophyte JunSE1L. We acknowledge institutional support from Utah State University.

During the preparation of this manuscript, the authors used ChatGPT (OpenAI) to assist with language editing and drafting of text. The authors have reviewed and edited the output and take full responsibility for the content of this publication.

 doi:10.20944/preprints202603.2503.v1

Conflicts of Interest: The authors declare no conflicts of interest. The funders had no role in the design of the study; in the collection, analyses, or interpretation of data; in the writing of the manuscript; or in the decision to publish the results.

Abbreviations

The following abbreviations are used in this manuscript:

ISR	Induced Systemic Resistance
H_2O_2	Hydrogen peroxide
LB	Lysogeny Broth
CFU	Colony Forming Units
SMA	Skim Milk Agar
OD	Optical Density
MM	Minimal Medium
RPM	Revolutions per minute
CMC	Critical Micelle Concentration
PCR	Polymerase Chain Reaction
UV	Ultraviolet
BLAST	Basic Local Alignment Search Tool
MAMPs	Microbe Associated Molecular Patterns

References

1. Truyens S, Weyens N, Cuypers A, Vangronsveld J. Bacterial seed endophytes: genera, vertical transmission and interaction with plants. Environ Microbiol Rep. 2015 Feb;7(1):40–50. https://doi.org/10.1111/1758-2229.12181
2. Bokhari A, Essack M, Lafi FF, Andres-Barrao C, Jalal R, Alamoudi S, et al. Bioprospecting desert plant Bacillus endophytic strains for their potential to enhance plant stress tolerance. Sci Rep. 2019 Dec 3;9(1):18154. https://doi.org/10.1038/s41598-019-54685-y
3. Sanz-Puente I, Redondo-Salvo S, Torres-Cortés G, De Toro M, Fernandes S, Börner A, et al. Seed-mediated vertical transmission of *Pantoea* core endophytes. ISME J. 2025 Jan 2;19(1):wraf192. https://doi.org/10.1093/ismejo/wraf192
4. Lopes R, Tsui S, Gonçalves PJRO, De Queiroz MV. A look into a multifunctional toolbox: endophytic Bacillus species provide broad and underexploited benefits for plants. World J Microbiol Biotechnol. 2018 Jul;34(7):94. https://doi.org/10.1007/s11274-018-2479-7
5. Pitzschke A. Developmental Peculiarities and Seed-Borne Endophytes in Quinoa: Omnipresent, Robust Bacilli Contribute to Plant Fitness. Front Microbiol. 2016 Jan 22;7. https://doi.org/10.3389/fmicb.2016.00002
6. Saxena AK, Kumar M, Chakdar H, Anuroopa N, Bagyaraj DJ. *Bacillus* species in soil as a natural resource for plant health and nutrition. J Appl Microbiol. 2020 Jun;128(6):1583–94. https://doi.org/10.1111/jam.14506
7. Etesami H, Jeong BR, Glick BR. Potential use of Bacillus spp. as an effective biostimulant against abiotic stresses in crops—A review. Curr Res Biotechnol. 2023;5:100128. https://doi.org/10.1016/j.crbiot.2023.100128
8. Valencia-Marin MF, Chávez-Avila S, Guzmán-Guzmán P, Orozco-Mosqueda MDC, De Los Santos-Villalobos S, Glick BR, et al. Survival strategies of Bacillus spp. in saline soils: Key factors to promote plant growth and health. Biotechnol Adv. 2024 Jan;70:108303. https://doi.org/10.1016/j.biotechadv.2023.108303
9. Dimkić I, Janakiev T, Petrović M, Degrassi G, Fira D. Plant-associated Bacillus and Pseudomonas antimicrobial activities in plant disease suppression via biological control mechanisms - A review. Physiol Mol Plant Pathol. 2022 Jan;117:101754. https://doi.org/10.1016/j.pmpp.2021.101754
10. Fira D, Dimkić I, Berić T, Lozo J, Stanković S. Biological control of plant pathogens by Bacillus species. J Biotechnol. 2018 Nov;285:44–55. https://doi.org/10.1016/j.jbiotec.2018.07.044

 doi:10.20944/preprints202603.2503.v1

11. Kiesewalter HT, Lozano-Andrade CN, Wibowo M, Strube ML, Maróti G, Snyder D, et al. Genomic and Chemical Diversity of Bacillus subtilis Secondary Metabolites against Plant Pathogenic Fungi. Traxler MF, editor. mSystems. 2021 Feb 23;6(1):e00770-20. https://doi.org/10.1128/mSystems.00770-20
12. Shafi J, Tian H, Ji M. *Bacillus* species as versatile weapons for plant pathogens: a review. Biotechnol Biotechnol Equip. 2017 May 4;31(3):446–59. https://doi.org/10.1080/13102818.2017.1286950
13. Chen W, Zhu B, Yang C, Wei C, He Y, Zheng L, et al. Decoupling Responses of Phyllosphere and Rhizosphere Bacterial Communities to Spatiotemporal Environmental Changes. Glob Change Biol. 2025 Apr;31(4):e70175. https://doi.org/10.1111/gcb.70175
14. Liu S, He F, Kuzyakov Y, Xiao H, Hoang DTT, Pu S, et al. Nutrients in the rhizosphere: A meta-analysis of content, availability, and influencing factors. Sci Total Environ. 2022 Jun;826:153908. https://doi.org/10.1016/j.scitotenv.2022.153908
15. Arnaouteli S, Bamford NC, Stanley-Wall NR, Kovács ÁT. Bacillus subtilis biofilm formation and social interactions. Nat Rev Microbiol. 2021 Sep;19(9):600–14. https://doi.org/10.1038/s41579-021-00540-9
16. Murugan PA, Sahu MK, Gupta MK, Sankar TS, Chandran S, Matheshwaran S. Deciphering the influence of NaCl on social behaviour of *Bacillus subtilis*. R Soc Open Sci. 2024 Sep;11(9):240822. https://doi.org/10.1098/rsos.240822
17. Rosazza T, Earl C, Eigentler L, Davidson FA, Stanley-Wall NR. Reciprocal sharing of extracellular proteases and extracellular matrix molecules facilitates *Bacillus subtilis* biofilm formation. Mol Microbiol. 2024 Aug;122(2):184–200. https://doi.org/10.1111/mmi.15288
18. Zaidi-Ait Salem M, Nait Chabane Y, Girbal-Neuhauser E. Architecture and physico-chemical properties of Bacillus amyloliquefaciens L-17 pellicle formed at the air–liquid interface. J Biosci Bioeng. 2021 Dec;132(6):560–8. https://doi.org/10.1016/j.jbiosc.2021.07.010
19. Zhang Y, Silva DM, Young P, Traini D, Li M, Ong HX, et al. Understanding the effects of aerodynamic and hydrodynamic shear forces on *Pseudomonas aeruginosa* biofilm growth. Biotechnol Bioeng. 2022 Jun;119(6):1483–97. https://doi.org/10.1002/bit.28077
20. Muhammad MH, Idris AL, Fan X, Guo Y, Yu Y, Jin X, et al. Beyond Risk: Bacterial Biofilms and Their Regulating Approaches. Front Microbiol. 2020 May 21;11:928. https://doi.org/10.3389/fmicb.2020.00928
21. Stoll A, Salvatierra-Martínez R, González M, Araya M. The Role of Surfactin Production by Bacillus velezensis on Colonization, Biofilm Formation on Tomato Root and Leaf Surfaces and Subsequent Protection (ISR) against Botrytis cinerea. Microorganisms. 2021 Oct 28;9(11):2251. https://doi.org/10.3390/microorganisms9112251
22. Stannius RO, Fusco S, Cowled M, Kovács ÁT. Surfactin accelerates Bacillus subtilis pellicle biofilm development.
23. Schenk HJ, Espino S, Romo DM, Nima N, Do AYT, Michaud JM, et al. Xylem Surfactants Introduce a New Element to the Cohesion-Tension Theory. Plant Physiol. 2017 Feb;173(2):1177–96. https://doi.org/10.1104/pp.16.01039
24. Khait I, Lewin-Epstein O, Sharon R, Saban K, Goldstein R, Anikster Y, et al. Sounds emitted by plants under stress are airborne and informative. Cell. 2023 Mar;186(7):1328-1336.e10. https://doi.org/10.1016/j.cell.2023.03.009
25. Hussain S, Tai B, Ali M, Jahan I, Sakina S, Wang G, et al. Antifungal potential of lipopeptides produced by the *Bacillus siamensis* Sh420 strain against *Fusarium graminearum*. Kovacs R, editor. Microbiol Spectr. 2024 Apr 2;12(4):e04008-23. https://doi.org/10.1128/spectrum.04008-23
26. Yuan Q, Yang P, Liu Y, Tabl KM, Guo M, Zhang J, et al. Iturin and fengycin lipopeptides inhibit pathogenic *Fusarium* by targeting multiple components of the cell membrane and their regulative effects in wheat. J Integr Plant Biol. 2025 Aug;67(8):2184–97. https://doi.org/10.1111/jipb.13933
27. Castaldi S, Petrillo C, Donadio G, Piaz FD, Cimmino A, Masi M, et al. Plant Growth Promotion Function of Bacillus sp. Strains Isolated from Salt-Pan Rhizosphere and Their Biocontrol Potential against Macrophomina phaseolina. Int J Mol Sci. 2021 Mar 24;22(7):3324. https://doi.org/10.3390/ijms22073324
28. Thérien M, Kiesewalter HT, Auria E, Charron-Lamoureux V, Wibowo M, Maróti G, et al. Surfactin production is not essential for pellicle and root-associated biofilm development of Bacillus subtilis. Biofilm. 2020 Dec;2:100021. https://doi.org/10.1016/j.bioflm.2020.100021

 doi:10.20944/preprints202603.2503.v1

29. Shahid I, Han J, Hanooq S, Malik KA, Borchers CH, Mehnaz S. Profiling of Metabolites of Bacillus spp. and Their Application in Sustainable Plant Growth Promotion and Biocontrol. Front Sustain Food Syst. 2021 Feb 22;5:605195. https://doi.org/10.3389/fsufs.2021.605195
30. Andrić S, Meyer T, Ongena M. Bacillus Responses to Plant-Associated Fungal and Bacterial Communities. Front Microbiol. 2020 Jun 23;11:1350. https://doi.org/10.3389/fmicb.2020.01350
31. Alvarez F, Castro M, Príncipe A, Borioli G, Fischer S, Mori G, et al. The plant-associated Bacillus amyloliquefaciens strains MEP218 and ARP23 capable of producing the cyclic lipopeptides iturin or surfactin and fengycin are effective in biocontrol of sclerotinia stem rot disease: Biocontrol of sclerotinia stem rot of soybean. J Appl Microbiol. 2012 Jan;112(1):159–74. https://doi.org/10.1111/j.1365-2672.2011.05182.x
32. Arnaouteli S, MacPhee CE, Stanley-Wall NR. Just in case it rains: building a hydrophobic biofilm the Bacillus subtilis way. Curr Opin Microbiol. 2016 Dec;34:7–12. https://doi.org/10.1016/j.mib.2016.07.012
33. Hobley L, Ostrowski A, Rao FV, Bromley KM, Porter M, Prescott AR, et al. BslA is a self-assembling bacterial hydrophobin that coats the *Bacillus subtilis* biofilm. Proc Natl Acad Sci. 2013 Aug 13;110(33):13600–5. https://doi.org/10.1073/pnas.1306390110
34. Kobayashi K, Iwano M. BslA(YuaB) forms a hydrophobic layer on the surface of *Bacillus subtilis* biofilms. Mol Microbiol. 2012 Jul;85(1):51–66. https://doi.org/10.1111/j.1365-2958.2012.08094.x
35. Ongena M, Jourdan E, Adam A, Paquot M, Brans A, Joris B, et al. Surfactin and fengycin lipopeptides of *Bacillus subtilis* as elicitors of induced systemic resistance in plants. Environ Microbiol. 2007 Apr;9(4):1084–90. https://doi.org/10.1111/j.1462-2920.2006.01202.x
36. Veening J, Igoshin OA, Eijlander RT, Nijland R, Hamoen LW, Kuipers OP. Transient heterogeneity in extracellular protease production by *Bacillus subtilis*. Mol Syst Biol. 2008 Jan;4(1):184. https://doi.org/10.1038/msb.2008.18
37. Schaeffer AB, Fulton MD. A Simplified Method of Staining Endospores. Science. 1933 Feb 17;77(1990):194–194. https://doi.org/10.1126/science.77.1990.194
38. Morris LS, Evans J, Marchesi JR. A robust plate assay for detection of extracellular microbial protease activity in metagenomic screens and pure cultures. J Microbiol Methods. 2012 Oct;91(1):144–6. https://doi.org/10.1016/j.mimet.2012.08.006
39. Bonebrake M, Anderson K, Valiente J, Jacobson A, McLean JE, Anderson A, et al. Biofilms Benefiting Plants Exposed to ZnO and CuO Nanoparticles Studied with a Root-Mimetic Hollow Fiber Membrane. J Agric Food Chem. 2018 Jul 5;66(26):6619–27. https://doi.org/10.1021/acs.jafc.7b02524
40. Frank JA, Reich CI, Sharma S, Weisbaum JS, Wilson BA, Olsen GJ. Critical Evaluation of Two Primers Commonly Used for Amplification of Bacterial 16S rRNA Genes. Appl Environ Microbiol. 2008 Apr 15;74(8):2461–70. https://doi.org/10.1128/AEM.02272-07
41. Vlamakis H, Chai Y, Beauregard P, Losick R, Kolter R. Sticking together: building a biofilm the Bacillus subtilis way. Nat Rev Microbiol. 2013 Mar;11(3):157–68. https://doi.org/10.1038/nrmicro2960
42. Lopez D, Vlamakis H, Kolter R. Biofilms. Cold Spring Harb Perspect Biol. 2010 Jul 1;2(7):a000398–a000398. https://doi.org/10.1101/cshperspect.a000398
43. Zhang N, Wang Z, Shao J, Xu Z, Liu Y, Xun W, et al. Biocontrol mechanisms of *Bacillus* : Improving the efficiency of green agriculture. Microb Biotechnol. 2023 Dec;16(12):2250–63. https://doi.org/10.1111/1751-7915.14348
44. Rychel K, Sastry AV, Palsson BO. Machine learning uncovers independently regulated modules in the Bacillus subtilis transcriptome. Nat Commun. 2020 Dec 11;11(1):6338. https://doi.org/10.1038/s41467-020-20153-9
45. Wei X, Pan Z, Chen Z, He N. Stress response regulation to extracellular polymeric substances biosynthesis in Bacillus licheniformis. Microb Cell Factories. 2025 Oct 14;24(1):222. https://doi.org/10.1186/s12934-025-02846-2
46. Huang Q, Zhang Z, Liu Q, Liu F, Liu Y, Zhang J, et al. SpoVG is an important regulator of sporulation and affects biofilm formation by regulating Spo0A transcription in Bacillus cereus 0–9. BMC Microbiol. 2021 Dec;21(1):172. https://doi.org/10.1186/s12866-021-02239-6

 doi:10.20944/preprints202603.2503.v1

47. Markelova N, Chumak A. Antimicrobial Activity of Bacillus Cyclic Lipopeptides and Their Role in the Host Adaptive Response to Changes in Environmental Conditions. Int J Mol Sci. 2025 Jan 2;26(1):336. https://doi.org/10.3390/ijms26010336
48. Soriano-Peña EY, Luna-Bulbarela A, Cristiano-Fajardo SA, Galindo E, Serrano-Carreón L. Modulation of the Sporulation Dynamics in the Plant-Probiotic Bacillus velezensis 83 via Carbon and Quorum-Sensing Metabolites. Probiotics Antimicrob Proteins. 2025 Oct;17(5):3743–62. https://doi.org/10.1007/s12602-025-10482-w
49. Bromley KM, Morris RJ, Hobley L, Brandani G, Gillespie RMC, McCluskey M, et al. Interfacial self-assembly of a bacterial hydrophobin. Proc Natl Acad Sci. 2015 Apr 28;112(17):5419–24. https://doi.org/10.1073/pnas.1419016112
50. Earl C, Arnaouteli S, Bamford NC, Porter M, Sukhodub T, MacPhee CE, et al. The majority of the matrix protein TapA is dispensable for *Bacillus subtilis* colony biofilm architecture. Mol Microbiol. 2020 Dec;114(6):920–33. https://doi.org/10.1111/mmi.14559
51. Raaijmakers JM, De Bruijn I, Nybroe O, Ongena M. Natural functions of lipopeptides from *Bacillus* and *Pseudomonas* : more than surfactants and antibiotics. FEMS Microbiol Rev. 2010 Nov;34(6):1037–62. https://doi.org/10.1111/j.1574-6976.2010.00221.x
52. Flemming HC, Wingender J. The biofilm matrix. Nat Rev Microbiol. 2010 Sep;8(9):623–33. https://doi.org/10.1038/nrmicro2415
53. Ahlawat OP, Yadav D, Kashyap PL, Khippal A, Singh G. Wheat endophytes and their potential role in managing abiotic stress under changing climate. J Appl Microbiol. 2022 Apr 1;132(4):2501–20. https://doi.org/10.1111/jam.15375
54. Kuźniar A, Włodarczyk K, Grządziel J, Woźniak M, Furtak K, Gałązka A, et al. New Insight into the Composition of Wheat Seed Microbiota. Int J Mol Sci. 2020 Jun 30;21(13):4634. https://doi.org/10.3390/ijms21134634
55. Mwita L, Chan WY, Pretorius T, Lyantagaye SL, Lapa SV, Avdeeva LV, et al. Gene expression regulation in the plant growth promoting Bacillus atrophaeus UCMB-5137 stimulated by maize root exudates. Gene. 2016 Sep;590(1):18–28. https://doi.org/10.1016/j.gene.2016.05.045
56. Akram W, Waqar S, Hanif S, Anjum T, Aftab Z e H, Li G, et al. Comparative Effect of Seed Coating and Biopriming of Bacillus aryabhattai Z-48 on Seedling Growth, Growth Promotion, and Suppression of Fusarium Wilt Disease of Tomato Plants. Microorganisms. 2024 Apr 14;12(4):792. https://doi.org/10.3390/microorganisms12040792
57. Rocha I, Ma Y, Souza-Alonso P, Vosátka M, Freitas H, Oliveira RS. Seed Coating: A Tool for Delivering Beneficial Microbes to Agricultural Crops. Front Plant Sci. 2019 Nov 6;10:1357. https://doi.org/10.3389/fpls.2019.01357
58. Kloepper JW, Ryu CM, Zhang S. Induced Systemic Resistance and Promotion of Plant Growth by *Bacillus* spp. Phytopathology®. 2004 Nov;94(11):1259–66. https://doi.org/10.1094/PHYTO.2004.94.11.1259